Controlling the evolution of two-dimensional electron gas states at a metal/Bi$_2$Se$_3$ interface

Han-Jin Noh,[1,*] Jinwon Jeong,[1] En-Jin Cho,[1] Joonbum Park,[2] Jun Sung Kim,[2] Ilyou Kim,[3]
Byeong-Gyu Park,[3] and Hyeong-Do Kim[4,5]

[1]*Department of Physics, Chonnam National University, Gwangju 500-757, Korea*
[2]*Department of Physics, Pohang University of Science and Technology, Pohang 790-784, Korea*
[3]*Pohang Accelerator Laboratory, Pohang University of Science and Technology, Pohang 790-784, Korea*
[4]*Center for Correlated Electron Systems, Institute for Basic Science (IBS), Seoul 151-747, Korea*
[5]*Department of Physics and Astronomy, Seoul National University, Seoul 151-747, Korea*

We demonstrate that the evolution of a two-dimensional electron gas system at an interface of a metal and the model topological insulator (TI) Bi$_2$Se$_3$ can be controlled by choosing an appropriate kind of metal element and by applying a low temperature evaporation procedure. In particular, we find that only topological surface states (TSSs) can exist at a Mn/Bi$_2$Se$_3$ interface, which would be useful for implementing a TI-based device with surface current channels only. The existence of TSSs alone at the interface is confirmed by angle-resolved photoemission spectroscopy (ARPES). Based on the ARPES and core-level x-ray photoemission spectroscopy measurements, we propose a cation intercalation model to explain our findings.

PACS number(s): 73.20.−r, 79.60.−i, 71.20.−b, 71.10.Pm

Since the discovery of topological insulators (TIs) with topologically protected metallic surface states [1–6], much attention has been paid to the characterization of topological surface states (TSSs), unveiling abundant exotic properties of TSSs, such as the absence of backscattering [7,8], spin-momentum locking [6,9], and their robustness against various kinds of surface perturbations [10–13]. In particular, studies on the effect of surface adsorbates on TSSs have found very intriguing phenomena, such as the fact that new Rashba-type spin-split surface states emerge on the (111) surface of a Bi$_2$Se$_3$ TI and that they have large amounts of common features irrespective of the electric and magnetic properties of the adsorbates [12,14,15]. Successive experimental and theoretical studies have suggested that the newly emerging surface states are actually interface states in a quantum-confined two-dimensional electron gas (2DEG) induced by a surface band-bending effect [16–18].

The coexistence of TSSs and 2DEG states is a very exotic example in the viewpoint of surface physics and have potential applications in the field of nanoscale spintronic devices [19], so the understanding of their origin and properties is essential in this TI physics. However, reports on the 2DEG states so far have focused on the evolution process, lacking in a controllability study. Since there are many practical reasons to control the 2DEG states depending on the implementation of TI-based devices, finding a controlling route of the 2DEG states at a metal/Bi$_2$Se$_3$ interface is crucial in this field.

In this Rapid Communication, we focus on this controllability of the 2DEG states and perform systematic angle-resolved photoemission spectroscopy (ARPES) measurements in order to explore whether there is a way to devolve the 2DEG states by leaving the TSSs alone at a metal/Bi$_2$Se$_3$ interface. Keeping in mind that the practicality of the surface states described above appears at an interface between a metal and TI, we deposit *in situ* several kinds of metal elements such as Cu, In, and

Mn on a (111) surface of Bi$_2$Se$_3$ in a well-controlled manner, which actually corresponds to an early stage of metal thin film synthesis, and observe an evolution and devolution of the TSSs and 2DEG states as a function of the deposition amount by ARPES and core-level x-ray photoemission spectroscopy (XPS). Our ARPES measurements reveal that in the case of Cu and In, the 2DEG states are developed with a Rashba-type spin-split electronic structure and are saturated up to ∼1 monolayer (ML), but that in the case of Mn, the 2DEG states are developed up to ∼0.4 ML, then disappear above ∼1.0 ML. In order to explain why Mn deposition makes a difference in Cu or In deposition, we keep track of the XPS spectral changes for Bi $4f$, Se $4d$, and Cu/In/Mn core levels, and propose a cation intercalation model where the intercalated cations act as a potential gradient reducer.

The typical features of TSSs in a fresh (111) surface of Bi$_2$Se$_3$ are presented in Fig. 1(a). The ARPES image was obtained along the $\overline{\Gamma}$-$\overline{K}$ direction within 15 min after cleaving the sample at 40 K, during which we did not observe any aging effect due to the adsorption of residual gas molecules in the vacuum chamber. This is quite different from the p-doped Bi$_2$Te$_3$ case in our previous report [2]. The V-shaped linear dispersive surface bands form two Dirac cones sharing a Dirac point (DP) located at around 200 meV below the Fermi level. Below the DP, a clear M-shaped bulk valence band is seen. On this cleaved surface, we deposited copper or indium atoms *in situ* by evaporating pure (99.999%) copper or indium metal with a well-controlled manner described in the Supplemental Material [20]. Figures 1(b)–1(d) show an evolution of the TSSs and the 2DEG states as a function of Cu deposition amount. At a small amount of Cu deposition (∼0.2 ML), newly developed surface states with Rashba-type spin splittings are clearly seen together with the TSSs. The DP and the M-shaped valence bands shift to the higher binding energy side by ∼0.3 eV. In Figs. 1(e)–1(h), a similar surface state evolution is displayed with an increase of In deposition. A prominent difference from the Cu deposition case appears in the size of the Rashba-type spin splittings, but both cases share common features in many aspects. The similar behavior of the surface state evolution has
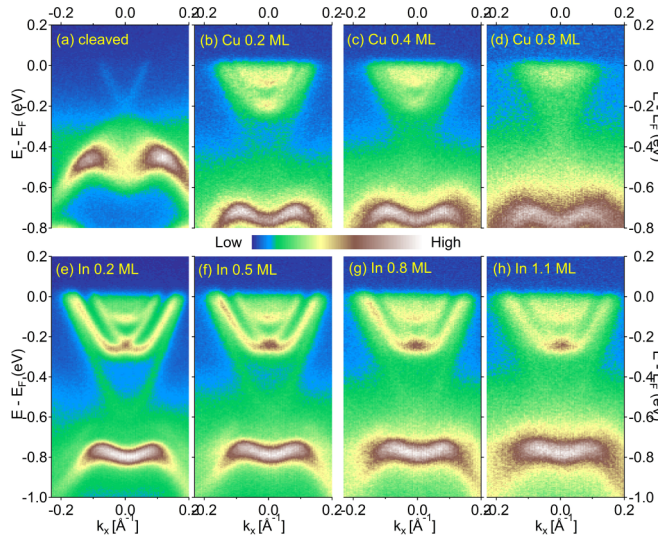
———————
*ffnhj@jnu.ac.kr

FIG. 1. (Color online) (a) ARPES-measured TSSs obtained from a clean (111) surface of Bi_2Se_3 along the $\overline{\Gamma}\text{-}\overline{K}$ direction within 15 min after *in situ* cleaving at 40 K. (b)–(d) ARPES images after 0.2, 0.4, and 0.8 ML Cu deposition, respectively. (e)–(h) ARPES images after 0.2, 0.5, 0.8, and 1.1 ML In deposition, respectively.

FIG. 2. (Color online) (a) ARPES-measured FSs (upper) and the dispersion relation of TSSs (lower) obtained from a clean (111) surface of Bi_2Se_3 along the $\overline{\Gamma}\text{-}\overline{M}$ direction within 1 h after *in situ* cleaving at 40 K. (b)–(d) The corresponding ARPES images after 0.2, 0.6, and 1.0 ML Mn deposition, respectively.

been reported for various kinds of surface deposition or surface adsorption [12,15]. However, the development of the surface states does not originate from a topological property of TIs but from an interface property of the metal/semiconductor. In the case of the $Bi_{0.9}Sb_{0.1}$ TI, our previous ARPES study shows just a small shift of the Fermi level in the electronic structure in response to the surface adsorption [11].

The origin of these surface states emerging in the (111) surface of Bi_2X_3 (X = chalcogen) compounds was initially controversial, but one of the most persuasive models argues that those are a kind of 2DEG state developed in a two-dimensional quantum well which is induced by a strong band bending at a metal/semiconductor interface [2,13,14,16,17]. According to this scenario, the dominant factors for the 2DEG states are the shape of the potential profile as a function of depth from the interface and the induced charge density at the interface, but the kinds and the amount of adsorbates are not important if only they stick on the surface to form a well-defined interface. Thus, in order to manipulate the 2DEG states at a metal/Bi_2Se_3 interface, or at least in order to make a surface electronic structure that is different than prototypical 2DEG states, metal elements that can intercalate or be interstitial defects are expected to be more effective. In this viewpoint, one different behavior between Cu and In depositions can be qualitatively understood. At a relatively thick deposition ($\gtrsim$0.8 ML), the 2DEG states appear more shrunken in the Cu-deposited sample than in the In-deposited sample, as shown in Figs. 1(d) and 1(g). This is possibly due to the intercalatability difference between Cu and In atoms for Bi_2Se_3. Actually, it has been reported that Cu atoms can intercalate into van der Waals (vdW) gaps in Bi_2Se_3, while a similar report for In atoms is missing, to our knowledge [21].

Keeping in mind that the intercalatability of the deposited atoms may be the crucial factor for our purpose, we chose Mn as a deposition material and kept track of the evolution
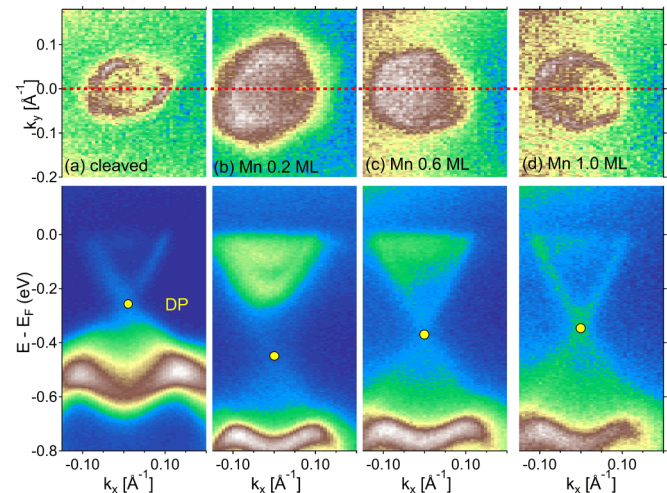
of 2DEG states as a function of deposition amount since it is known that a small amount of Mn can be doped in Bi_2Se_3 [22]. Rubidium was also reported to intercalate into the gap, but its effect on the 2DEG states lies in another direction to our purpose [23]. Figures 2(a)–2(d) show the ARPES-measured Fermi surface (upper panel) and the corresponding energy dispersion relation (lower panel) along the dotted red line (approximately $\overline{\Gamma}\text{-}\overline{M}$ direction) for a clean surface, and 0.2, 0.6, and 1.0 ML Mn-deposited surfaces, respectively. Interestingly enough, Mn-deposited surfaces show a very different evolution of the 2DEG states. At a small amount of Mn deposition ($\sim$0.2 ML), a quite complex 2DEG structure is developed, as shown in Fig. 2(b). It appears similar to that of the Cu-deposited surface. However, when the deposition amount is larger than $\sim$0.2 ML, the Fermi surface (FS) size of the 2DEG states becomes smaller, and the DP shifts up by $\sim$0.1 eV, as is shown in Fig. 2(c). At around 1.0 ML Mn, the 2DEG states almost disappear and only the TSSs remain, as can be seen in Fig. 2(d). Based on the facts that the energy position of the DP in 1.0 ML Mn deposition is $\sim$0.1 eV deeper than that of the clean surface, and that the size of the hexagonal FS of the TSSs is a little larger than that of the clean surface, the surface does not recover to its original condition, but forms another interface that gives a similar environment to the original vacuum/(111) interface for the TSSs and 2DEG.

In order to figure out why the Mn deposition causes such intriguing behavior in the evolution of 2DEG states, we carried out core-level XPS measurements, as displayed in Fig. 3. Since XPS is sensitive to the chemical valency and chemical environment of ions in solids, important information or at least a clue on the reason for the disappearance of the 2DEG states can be obtained by analyzing the XPS spectra. In the left column, the center one, and the right one of Fig. 3, the XPS spectra of each deposited element core level, Bi $4f$, and Se $3d$ level are presented with an increase of the deposition amount, respectively. In the case of In deposition, the Bi $4f_{5/2,7/2}$ and
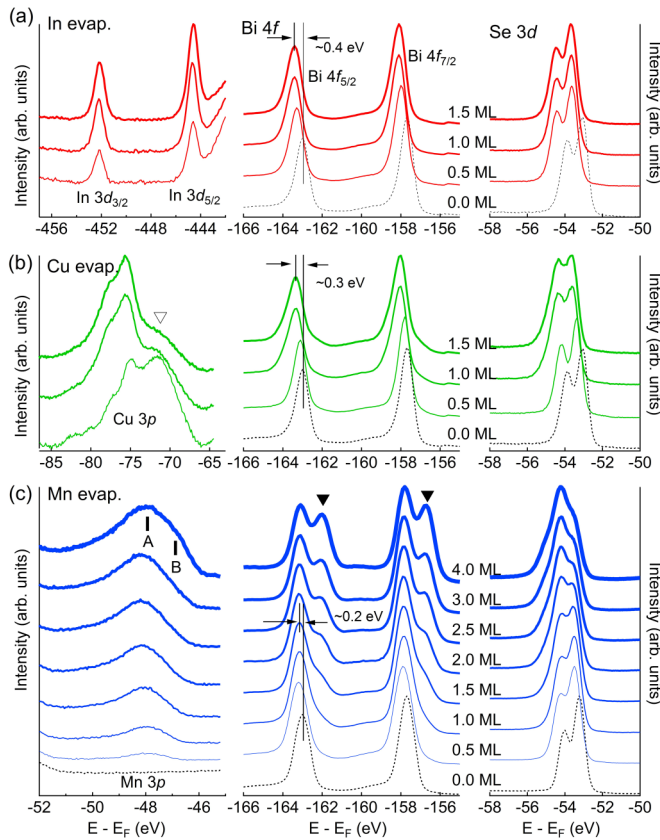
FIG. 3. (Color online) (a) Core-level XPS spectra of In $3d$ (left column), Bi $4f$ (center column), and Se $3d$ (right column) on the (111) surface of Bi_2Se_3 with an increase of the deposition amount. (b) Cu case. (c) Mn case.

Se $3d_{3/2,5/2}$ peaks shift toward the lower kinetic energy side by $\sim$0.4 eV with an increase of the deposition amount, as shown in Fig. 3(a). The amount of the energy shift corresponds to the band bending shown in Figs. 1(a) and 1(h), so it can be interpreted as a surface potential shift due to the accumulated surface charge induced by the In deposits. Similar core-level shifts are observed in the Cu- and Mn-deposited surfaces, respectively, as is shown in Figs. 3(b) and 3(c), and the amount of energy shift is also very consistent with that of the band shift in Figs. 1 and 2.

Several interesting features in the core-level spectra of each deposited element, Bi $4f$, and Se $3d$ are found in a different dependence on deposition. While In deposition does not cause any change in the In $3d$, Bi $4f$, and Se $3d$ spectral line shape, Cu(Mn) deposition induces an evolution in the Cu $3p$ (Mn $3p$), Bi $4f$, and Se $3d$ levels, respectively. In the Cu $3p$ region, two doublets (75 and 71 eV) are observed, each of which can be assigned to the surface peak and intercalation peak ($\bigtriangledown$), as shown in Fig. 3(b). The relative peak weight dependence on deposition amount strongly supports this assignment, and a similar result has been reported in a Rb deposition/annealing study [23]. Meanwhile, Mn $3p$ does not cause as prominent a difference as does Cu $3p$, but a quantitative peak analysis reveals that below $\sim$1.5 ML, the deposited Mn atoms mostly form Mn^{3+} ions [peak A in Fig. 3(c)] either at the interface or at the intersites, but that above $\sim$1.5 ML, a portion of the

Mn^{2+} ions (peak B) starts to increase with clustering of the deposited Mn atoms and reaches $\sim$70% at $\sim$4.0 ML [20]. For both Cu and Mn deposition cases, a new doublet of Se $3d$ appears at a $\sim$0.5 eV lower kinetic energy than that of the main peak, together with an increase of the peak width. This indicates an occurrence of another kind of Se ion that is chemically different from those in pristine Bi_2Se_3. Similar evolutionary behavior is observed in the Bi $4f$ region ($\blacktriangledown$) of Fig. 3(c). The prominent evolution of the Bi $4f$ peaks in the Mn-deposited surface is quite contrastive to the Cu case where the Bi $4f$ peaks hardly show a dependence on the Cu deposition amount. Further quantitative information on the XPS spectra is available in the Supplemental Material [20].

The element-specific response to the deposits indicates that intercalatability and intercalated sites of the deposits into Bi_2Se_3 bulk are different for In, Cu, and Mn. The invariance of the XPS spectra in the In-deposited surface suggests that In atoms do not intercalate into the Bi_2Se_3 bulk. Meanwhile, a part of the Cu or Mn deposits definitely intercalates into the bulk, but their intercalated sites are different. Based on the Bi $4f$ and Se $3d$ XPS spectra, the intercalated Cu atoms affect the Se anions only. Meanwhile, the intercalated Mn atoms affect the Bi ions as well as the Se ions. This contrastive response suggests that the intercalated Cu atoms reside mainly in the vdW gaps between the quintuple layers (QLs) while the Mn atoms are in the interstitial sites. This also explains why the binding energy of the intercalated Cu $3p$ levels is smaller than that of the deposited Cu on the surface. Since the QLs are chemically very stable and electrically close to neutral, the intercalated atoms in the vdW gaps are also very close to charge neutral, so the binding energy of the atoms is smaller than that of the Cu metal, which is close to a monovalent ion. The zero valence of the intercalated Cu ions in the vdW gaps of Bi_2Se_3 has been reported in an electron energy
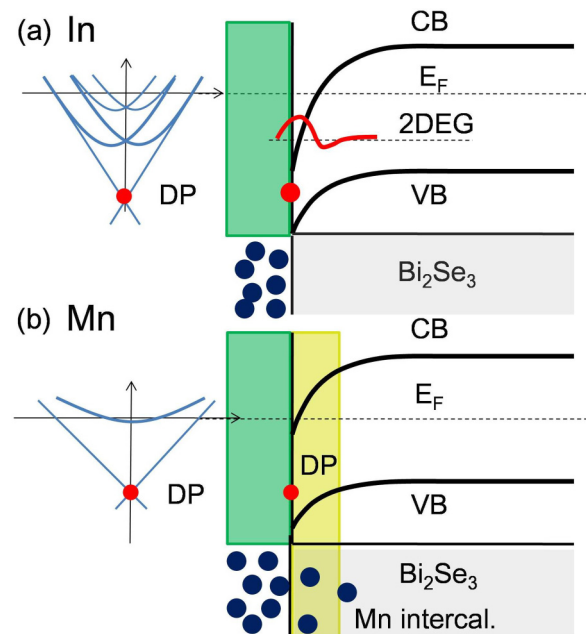

FIG. 4. (Color online) Schematic band alignments for the interfaces of (a) In/Bi_2Se_3 and (b) Mn/Bi_2Se_3.

loss spectroscopy study [24]. Meanwhile, the interstitial Mn atoms are likely to act as cations, as do Bi atoms. The Mn $3p$ XPS spectra in Fig. 3(c) support this interpretation. If this is the case, the intercalated Mn cations cannot help moderating the surface band-bending effect induced by the deposited Mn adsorbates.

The XPS measurements described above give important information to explain the appearance and disappearance of 2DEG states in our ARPES data. Probably the most simple way to remove 2DEG is to weaken the adsorbate-induced band bending at the interface. We have evidenced in the XPS study that the Mn adsorbates intercalate into the interstitial sites of Bi_2Se_3. If the intercalated Mn gives a few electrons per atom that act as Mn cations, the surface potential gradient gets smaller as the average intercalation depth gets larger. Figures 4(a) and 4(b) show a schematic configuration for our cation intercalation model. In the case of In deposition, the surface charges induced by the deposited indium ions attract electrons toward the In/Bi_2Se_3 interface, making a 2DEG system. When there are no intercalating indium ions, a deep well-like surface potential forms at the interface, developing 2DEG states with a complex Rashba-type spin-splitting structure. However, as in the case of Mn deposition, if

parts of the deposited Mn atoms intercalate into the interstitial sites of Bi_2Se_3, and are ionized into Mn cations, the deep well-like surface potential changes to a wide valley with a gentle slope. In this model, the different response to Cu deposition is also naturally explained. As is described above, Cu atoms are also known to intercalate into the vdW gap, but they do not intercalate into the interstitial sites, so almost all of the intercalated Cu atoms stay charge neutral. The lower binding energy of the intercalated Cu $3p$ peak in Fig. 3(b) supports this interpretation. Actually, if we compare the Cu and In deposition results, the 2DEG states in the Cu deposition shrink a little more than those in the In deposition [see Figs. 1(d) and 1(g)]. So, the Cu intercalation effects definitely exist, but are not as prominent as in the Mn case due to the zero valence of the intercalated Cu ions.

[1] L. Fu, C. L. Kane, and E. J. Mele, Phys. Rev. Lett. **98**, 106803 (2007).

[2] H.-J. Noh, H. Koh, S.-J. Oh, J.-H. Park, H.-D. Kim, J. D. Rameau, T. Valla, T. E. Kidd, P. D. Johnson, Y. Hu, and Q. Li, Europhys. Lett. **81**, 57006 (2008).

[3] D. Hsieh, D. Qian, L. Wray, Y. Xia, Y. S. Hor, R. J. Cava, and M. Z. Hasan, Nature (London) **452**, 970 (2008).

[4] Y. Xia, D. Qian, D. Hsieh, L. Wray, A. Pal, H. Lin, A. Bansil, D. Grauer, Y. S. Hor, R. J. Cava, and M. Z. Hasan, Nat. Phys. **5**, 398 (2009).

[5] H. Zhang, C.-X. Liu, X.-L. Qi, X. Dai, Z. Fang, and S.-C. Zhang, Nat. Phys. **5**, 438 (2009).

[6] D. Hsieh, Y. Xia, L. Wray, D. Qian, A. Pal, J. H. Dil, J. Osterwalder, F. Meier, G. Bihlmayer, C. L. Kane, Y. S. Hor, R. J. Cava, and M. Z. Hasan, Science **323**, 919 (2009).

[7] P. Roushan, J. Seo, C. V. Parker, Y. S. Hor, D. Hsieh, D. Qian, A. Richardella, M. Z. Hasan, R. J. Cava, and A. Yazdani, Nature (London) **460**, 1106 (2009).

[8] T. Zhang, P. Cheng, X. Chen, J.-F. Jia, X. Ma, K. He, L. Wang, H. Zhang, X. Dai, Z. Fang, X. Xie, and Q.-K. Xue, Phys. Rev. Lett. **103**, 266803 (2009).

[9] Z.-H. Pan, E. Vescovo, A. V. Fedorov, D. Gardner, Y. S. Lee, S. Chu, G. D. Gu, and T. Valla, Phys. Rev. Lett. **106**, 257004 (2011).

[10] S. R. Park, W. S. Jung, C. Kim, D. J. Song, C. Kim, S. Kimura, K. D. Lee, and N. Hur, Phys. Rev. B **81**, 041405 (2010).

[11] H.-J. Noh, J. Jeong, E.-J. Cho, H.-K. Lee, and H.-D. Kim, Europhys. Lett. **96**, 47002 (2011).

[12] T. Valla, Z.-H. Pan, D. Gardner, Y. S. Lee, and S. Chu, Phys. Rev. Lett. **108**, 117601 (2012).

[13] L. A. Wray, S.-Y. Xu, Y. Xia, D. Hsieh, A. V. Fedorov, Y. S. Hor, R. J. Cava, A. Bansil, H. Lin, and M. Z. Hasan, Nat. Phys. **7**, 32 (2011).

[14] P. D. C. King, R. C. Hatch, M. Bianchi, R. Ovsyannikov, C. Lupulescu, G. Landolt, B. Slomski, J. H. Dil, D. Guan, J. L. Mi, E. D. L. Rienks, J. Fink, A. Lindblad, S. Svensson, S. Bao, G. Balakrishnan, B. B. Iversen, J. Osterwalder, W. Eberhardt, F. Baumberger, and Ph. Hofmann, Phys. Rev. Lett. **107**, 096802 (2011).

[15] H. M. Benia, C. Lin, K. Kern, and C. R. Ast, Phys. Rev. Lett. **107**, 177602 (2011).

[16] M. Bianchi, D. Guan, S. Bao, J. Mi, B. B. Iversen, P. D. C. King, and Ph. Hofmann, Nat. Commun. **1**, 128 (2010).

[17] M. S. Bahramy, P. D. C. King, A. de la Torre, J. Chang, M. Shi, L. Patthey, G. Bakakrishnan, Ph. Hofmann, R. Arita, N. Nagaosa, and F. Baumberger, Nat. Commun. **3**, 1159 (2012).

[18] C. Mann, D. West, I. Miotkowski, Y. P. Chen, S. Zhang, and C.-K. Shih, Nat. Commun. **4**, 2277 (2013).

[19] S. Datta and B. Das, Appl. Phys. Lett. **56**, 665 (1990).

[20] See Supplemental Material at http://link.aps.org/supplemental/10.1103/PhysRevB.91.121110 for additional information on experimental details and curve fittings of the XPS spectra.

[21] Y.-L. Wang, Y. Xu, Y.-P. Jiang, J.-W. Liu, C.-Z. Chang, M. Chen, Z. Li, C.-L. Song, L.-L. Wang, K. He, X. Chen, W.-H. Duan, Q.-K. Xue, and X.-C. Ma, Phys. Rev. B **84**, 075335 (2011).

[22] J. Choi, H.-W. Lee, B.-S. Kim, H. Park, S. Choi, S. C. Hong, and S. Cho, J. Magn. Magn. Mater. **304**, e164 (2006).

[23] M. Bianchi, R. C. Hatch, Z. Li, P. Hofmann, F. Song, J. Mi, B. B. Iversen, Z. M. A. El-Fattah, P. Löptien, L. Zhou, A. A. Khajetoorians, J. Wiebe, R. Siesendanger, and J. W. Wells, ACS Nano **6**, 7009 (2012).

[24] K. J. Koski, J. J. Cha, B. W. Reed, C. D. Wessells, D. Kong, and Y. Cui, J. Am. Chem. Soc. **134**, 7584 (2012).